Sustainable Structures
ISSN: 2789-3111 (Print); ISSN: 2789-312X (Online)
http://www.sustain-dpl.com/journal/sust
DOI: 10.54113/j.sust.2024.000046

ORIGINAL ARTICLE

Investigating crack growth in two-dimensional plates with openings using the peri-dynamic method

Mohammad Norouzi Shavir [a], Pouria Biglari [b], Navid Mirzaii [b], Reza Rashmehkarim [c], Peyman Beiranvand [d,*]

[a] School of Civil Engineering, College of Engineering, University of Tehran, Tehran, Iran.
[b] School of Civil Engineering, Iran University of Science and Technology, Narmak, Tehran, Iran.
[c] Faculty of Mechanical and Mechatronics Engineering, Shahrood University of Technology, Iran.
[d] School of Civil Engineering, Iran University of Science and Technology, Narmak, Tehran, Iran.
[*]Corresponding Author: Peyman Beiranvand. Email: peyman51471366@gmail.com

Abstract: Analyzing and simulating the growth of dynamic cracks in the shell of structures and two-dimensional plates is one of the important topics for providing solutions to prevent crack growth and sudden failures, which increases the lifespan of the structure. Despite many studies by researchers regarding the behavior of structures against crack growth and sudden failure, there are still many problems regarding the analysis and simulation of the mechanical behavior of shells and plates with openings. Therefore, the peri-dynamic method can be directly used to model crack growth in these types of structures. In this research, modeling of dynamic crack growth as well as factors affecting crack growth and branching in the shell of structures (with and without openings) were investigated using the peri-dynamic method in LAMMPS software. Then the results obtained from the pre-dynamic method were verified with the results of other methods. The comparison of different results showed that the peri-dynamics method is capable of properly modeling crack growth in plates and shells with openings, and in other words, this theory can predict the path of crack growth with high accuracy. According to the obtained results, it can be stated that the process of crack growth and branching in the shell of structures depends on values such as the applied stress, the type of material and the direction of the fibers in the composites, as well as the absence of openings in the shell, which by changing these factors, the speed and The path of crack growth in the body of the structure changes.

Keywords: Crack growth; Peri-dynamic method; Shell structures; Openings; LAMMPS.

1 Introduction

The prevention of sudden fracture in structures is of significant importance in the industry and consequently analyzing and modeling fracture and crack growth in different structures are essential. The lifetime of parts can be improved if the path of damage and crack growth is predicted, controlled, and directed in a specific way. Many research have been performed in this field. Generally, the theories and methods used to analyze the fracture and crack growth in bodies can be divided into two categories. The first one has been presented based on the classical theory of solid mechanics called continuous medium theory, and the second is based on molecular dynamics theory. Both approaches have their advantages and drawbacks. For example, the principle of mathematical formulation in continuous medium theory is derived from the partial differential equation and therefore it cannot be used directly

Received: 5 May 2024; Received in revised form: 24 August 2024; Accepted: 26 August 2024

to analyze and model points of singularity and discontinuities in the geometry. In this approach, finite element methods (FEM) are widely used which specify the initial location of the crack and its growth path and therefore make them highly dependent on the type of mesh and its geometry. On the other hand, methods and models employed in the molecular dynamic theory also have some issues such as small longitudinal and temporal scales. The one problem is the small longitudinal scale applied in the molecular dynamic theory compared to actual dimensions of structures and another is very short term of the temporal scale used in these models. Therefore, a very high loading rate is used in the molecular dynamic simulation which is far from reality. Such restrictions on conventional methods for the analysis of damage, failure, and crack growth in structures with points of singularity and discontinuities are the driving forces for research and innovation in the field.

Silling (2000) [1] proposed the formulation called Peri-dynamic (PD) to model discontinuities in materials. He discussed the propagation of linear stress waves in the new theory and derived wave propagation relations. In this approach, no need to use special mathematical techniques at the points where the discontinuities occur to model discontinuities of various types. This theory formulates problems in terms of integral equations rather than partial differential equations. The points of singularity and discontinuities and damage in bodies and their modeling are another type of deformation and part of the structural equation in PD theory. In other words, in PD theory, there is no distinction between points in a body that have discontinuous displacement or derivative of displacement. As a result, without the need for complementary relationships, PD theory is used directly to model fracture and crack growth in problems with bodies and structures having points of singularity and discontinuities. PD theory equations are extended with the concept of coherence in a finite distance called the horizon line (δ) and are expressed based on a model for internal forces among the particles in the body in which the material points (particles) apply force directly on each other on a close distance. While the classical theory of solid mechanics is based on the continuous distribution of mass in a body, assuming that all internal forces are contact forces exerted by two particles on each other, at a zero distance from each other (two adjacent particles). Given the above, the classical theory of solids mechanics can be considered a special case of PD theory. When the value of the horizon line (d) is reduced to zero in PD theory ($\delta \rightarrow 0$), PD theory converges to the classical theory of solids mechanics.

In the recent decade, PD theory has attracted the interest of researchers in computational solid mechanics to analyze and model fracture, crack growth, and damage in structures under various loading and structural conditions [2–4]. Silling and Askari [5] proposed a mesh less method based on PD theory to solve numerically dynamic problems. They also discussed the stability and accuracy of PD theory and, by studying several examples, revealed the characteristics of this theory in modeling brittle dynamic crack growth. Kilic and Madenci [6] considered two sets of problems to study buckling characteristics of PD theory. The rectangular columns under compression were utilized to evaluate the impact of boundary conditions and the cross-sectional area on buckling load. On the other hand, to determine the influence of plate dimension and material properties on the critical buckling temperature, a uniform temperature load was exerted on rectangular plates. The implementation of PD theory within the framework of molecular dynamics code in AMU software as well as in LAMMPS software [7, 8] by Silling et al. was another study in the developing PD theory that added computational mechanics capability to MD code.

Silling et al. [9] developed PD theory and presented a generalization of the bond-based Peri-dynamic theory. They have divided it into three types of formulations including bond-based Peri-dynamics, ordinary state-based Peri-dynamics, and non-ordinary state-based Peri-dynamics. In the first model, there was linear bonding force employed two material points x and x', in addition, the magnitude of the force applied on the material point x' by the material point x and vice versa were equal. The second model was ordinary state-based PD theory that the force applied between the two material points x and x' was along the line contacting those two points just like the first model, nevertheless, the magnitude of force exerted on each other by two different points was not equal. In the third model, in addition to the fact that the force exerted by two points is not equal, the force exerted between the two material points x and x' may also be in any direction.

Ren et al. [10] introduced a dual-horizon Peri-dynamics (DH-PD) formulation. This concept has been presented to study the unbalanced interactions between the particles with different horizon sizes.

They indicated that their framework could implement all three Peri-dynamic formulations. Ha and Bobaru [11– 13] modeled the crack growth and dynamic brittle fracture using the bond-based PD theory to evaluate effective parameters on crack growth in the body. They considered the effect of stress intensity and mechanical properties on crack growth process and branching of crack growth path in the body. In this study, the results of modeling crack growth by PD theory were in good agreement with the experimental results, which shows its ability to analyze and model crack growth and damage in the body.

Agwai et al. [14] compared PD theory with other conventional numerical methods of crack growth modeling. However, PD theory showed closer findings to experimental observations with higher accuracy in predicting the path of crack growth and fracture in the body. Zhou et al. [15] investigated the initiation, propagation, and coalescence of cracks in the Brazilian Disk specimens using the non-ordinary state-based Peri-dynamics. It was shown that PD theory was able to model crack growth in various problems without changing the criterion proving its accuracy. Zhao et al. [16] provided a comparison between PD theory and XFEM in crack growth modeling based on the results of two examples. In the first example, crack propagation in a double-notched sample was modeled. This sample was under uniaxial tensile stress with various cracks. In the second one, samples had two center cracks. Both PD and XFEM showed close results. Later, Giannakeas et al. [17] developed a PD–extended XFEM coupling strategy for brittle fracture simulation. Shafiei [18] studied the crack path for inclined crack under dynamic loading. Peri-dynamic solution was presented to show crack generation and crack branching. Furthermore, the effect of pre-crack angle and the stress value applied on the desired plate on the manner of crack growth was examined. In another work, Sealing and Askari [19], evaluated PD theory in fatigue crack propagation modeling. It is revealed that the presented model reproduces the main features of S-N data for typical materials. They demonstrated the nucleation and growth of a helical fatigue crack in an aluminum alloy sample under torsion through 3D example. Basoglu et al. [20] modeled crack growth and examined the effect of small cracks on crack growth propagation caused by initial pre-crack in the body. Karpenko et al. [21] applied an ordinary state-based Peri-dynamics (SBPD) model to study and analyze the impact of small holes and micro-cracks in concrete structures based on toughening and degradation mechanisms. The PD simulation agreed well with analytical solutions indicating its capability and efficiency to find the paths of complex crack propagation.

Recently, many other applications of PD theory have been developed including correspondence model for creep in metals and solving static problems [22], simulation of crack propagation during the SCB testing process [23]; studies and simulation of thermal failure behaviors in bodies under thermal stress, thermal cycling treatment, and thermal shock [24–26]; analysis and modeling of progressive damage and delamination growth in composite laminates [27–29]; analyzing crack growth and damage in hyper elastic materials [30], viscoelastic materials [31], and heterogeneous materials [32]; and buckling analysis of cracked plates [33] and dynamic brittle fracture in glass [34].

The purpose of the present study is to evaluate the PD theory in modeling crack growth in composite, bi-material, and isotropic plates with inclusion. In the first section of the study, a review of previous studies and researches conducted by researchers in the field of PD theory is provided. In the second section, the basis and formulation of the PD theory are presented. The third section is related to numerical examples and modeling of crack growth. And finally, the study is concluded.

2 Peri-dynamic theory

Each body and structure in PD theory consists of a large number of material points (particles) that each of them has a specific position at a given time. PD theory analyzes the motion and deformation of the body, taking into account the interaction between the material point $x_{(k)}$ and many other possible material points (particles) of the body, such as $x_{(j)}$ $(j = 1,2,3, \dots, \infty)$. Therefore, there is an infinite number of interactions between material points $x_{(k)}$ and other material points. In PD theory, it is assumed that the field of interaction of the material point $x_{(k)}$ with other material points is determined by the horizon line δ $(\delta > 0)$, moreover, all the material points which are at a distance less than the horizontal line (δ) from point $x_{(k)}$, are called the family or the neighborhood of $x_{(k)}$ and are

represented by $\mathcal{H}_{x_{(k)}}$, and it is also assumed that the effect of material points in the interaction with the material point $x_{(k)}$ disappear in the region beyond the family area of $\mathcal{H}_{x_{(k)}}$. The interaction of the material point *x* with another material point x' inside the family $\mathcal{H}_x$ is represented by the vectorξ, which is called the bond vector. Therefore, there is an infinite number of bonding between the material point x and the material points within its family. Given the aforementioned issues, the family of the material point *x* is defined using the following relation [4]:

$$\boldsymbol{\mathcal{H}_x = \{x' \epsilon B | 0 < |x' - x| \leq \delta\}} \quad (1)$$

The equation of motion for a continuous media for use in PD model is presented as follows:

$$\boldsymbol{\rho(x)\ddot{u}(x,t) = \int_{\mathcal{H}_x} f(\xi, \eta\ )dv_{\mathcal{H}_x} + b(x,t)} \quad (2)$$

Where $\mathcal{H}_x$ denotes the area in the family and neighborhood *x* and *u* is a displacement vector and $b(x,t)$ is a volume force vector. Here, f is called the pairwise force function, which represents the reciprocal vector between x and x'.

The concept of the neighborhood of the material point *x* as well as the concept of the bond vector between the two material points is illustrated in **Fig.1**.

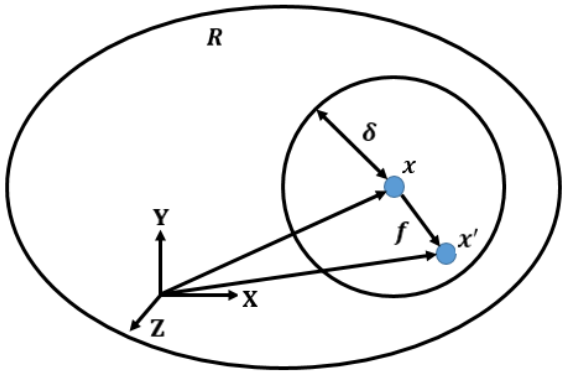

Fig. 1. Family of material point x.

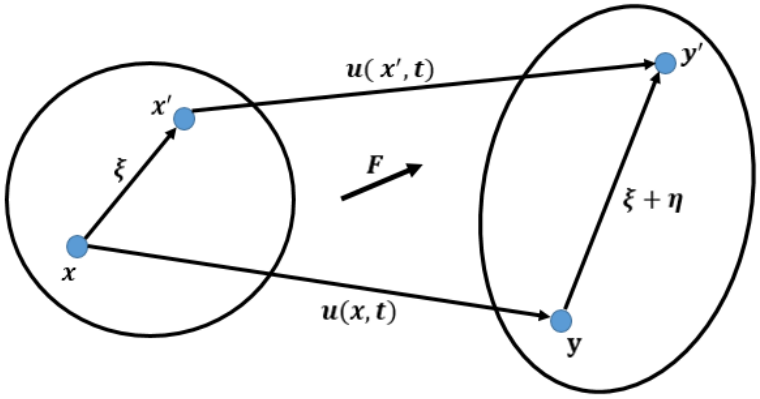

$$\boldsymbol{y = x + u(x,t), \quad y' = x' + u(x',t)}$$
$$\boldsymbol{\xi = x' - x, \quad \eta = \ = u(x',t) - u(x,t)}$$

Fig. 2. Schematic description of coordinates and deformation of body in the reference and deformed configurations.

According to Fig. 2, the position of the material point x relative to x' is denoted by the vector ξ and η represents the displacement vector of the aforementioned two points relative to each other.

$$\boldsymbol{\xi = x' - x} \quad (3)$$

$$\boldsymbol{\eta = u(x',t) - u(x,t)} \quad (4)$$

In relation (4), $u(x,t)$ and $u(x',t)$ are the displacement vectors of material points x and x' with respect to the reference configuration (configuration of the body before the deformation), respectively, and the vector $\xi + \eta$ represents the relative position vector of the two material points x

and x' in the present configuration. One of the basic concepts in PD theory is that, after the deformation of the reference configuration, in addition to the deformation of the bond vector between the material points, the family of the material point *x* also changes. The concept of deformation of the bond vector and the family of the material point *x* after the deformation of the reference configuration, as well as the vectors $u(x,t)$ and $u(x',t)$, which respectively indicate the displacement vectors of the material points x and x', are demonstrated in **Fig.2**.

As mentioned earlier, points that are outside the horizon line of the material point *x*, have no bonding with the material point *x*. In other words, the value of the bonding force ($f(\eta,\xi)$) between the material point *x* and the material point outside the horizon line (neighborhood) of the material point *x* is zero [4]:

$$|\boldsymbol{\xi}| > \boldsymbol{\delta} \rightarrow \boldsymbol{f}(\boldsymbol{\eta},\boldsymbol{\xi}) = \mathbf{0}, \quad \forall \quad \boldsymbol{\xi},\boldsymbol{\eta} \tag{5}$$

The third law of Newton and the condition for the conservation of the linear and angular momentum determines the general form of the pairwise force function (*f*) among the material points. According to this law, the force that the material point *x* applies to the material point x' is equal to and in the opposite direction to the force that the material point x' exerts on the material point *x*, therefore [4]:

$$\boldsymbol{f}(-\boldsymbol{\eta},\boldsymbol{\xi}) = -\boldsymbol{f}(\boldsymbol{\eta},\boldsymbol{\xi}), \quad \forall \quad \boldsymbol{\xi},\boldsymbol{\eta} \tag{6}$$

It should be noted that relation (6) satisfies the condition of the conservation of the linear momentum on the pairwise force vector (*f*) between the two material points *x* andx'. Using the law of conservation of the angular momentum:

$$(\boldsymbol{\xi}+\boldsymbol{\eta}) \times \boldsymbol{f}(\boldsymbol{\eta},\boldsymbol{\xi}) = \mathbf{0}, \quad \forall \quad \boldsymbol{\xi},\boldsymbol{\eta} \tag{7}$$

According to relation (7), it can be stated that the force vector between two material points in PD theory is parallel to their relative position vector in the present configuration (after deformation). For linear isotropic materials, the pairwise force function in the bond vector between material points is defined as follows:

$$\boldsymbol{f}(\boldsymbol{\eta},\boldsymbol{\xi}) = \boldsymbol{cs}\frac{\boldsymbol{\partial}|\boldsymbol{\xi}+\boldsymbol{\eta}|}{\boldsymbol{\partial\eta}} \tag{8}$$

In relation (8), *c* is the material micro-module in PD theory, which relies on the type and structure of the material, and *s* is the relative change in the length of the bond vector between the two material points in the body defined in the following form:

$$\boldsymbol{s} = \frac{|\boldsymbol{\eta}+\boldsymbol{\xi}| - |\boldsymbol{\xi}|}{|\boldsymbol{\xi}|} \tag{9}$$

The coefficient c, which determines the materials in the PMB model can be presented as follows:

$$c = \frac{18k}{\pi\delta^4} \qquad for\ 3D \tag{10}$$

$$c = \frac{6E}{\pi\delta^3(1-v)} \qquad for\ 2D \tag{11}$$

The values of fracture toughness,G_0, for a fractured surface in PD theory is obtained as:

$$G_{0_{3D}} = \int_0^{\delta}\int_0^{2\pi}\int_0^{\delta}\int_0^{cos^{-1}\ z/\xi}\left(\frac{cs_0{}^2\xi}{2}\right)sin\emptyset d\emptyset d\xi d\theta dz = \frac{\pi\ cs_0^2\delta^5}{10} \qquad for\ 3D \tag{12}$$

$$G_{0_{2D}} = 2t\int_0^{\delta}\int_0^{\delta}\int_0^{cos^{-1}\ z/\xi}\left(\frac{cs_0{}^2\xi}{2}\right)sin\emptyset d\emptyset d\xi dz = \frac{\pi\ cs_0^2 t\delta^4}{4} \qquad for\ 2D \tag{13}$$

Therefore, the critical bond tension of s_0 in 2D and 3D is determined as follows:

$$s_0 = \sqrt{\frac{10G_0}{\pi c \delta^{\,5}}} = \sqrt{\frac{5\pi G_0}{9k\delta}} \qquad for\ \ 3D \tag{14}$$

$$s_0 = \sqrt{\frac{4\pi G_0}{9E\delta}} \qquad for\ \ 2D \tag{15}$$

Material damage in PD theory is defined by breaking the bond vector between the material points and, consequently, the destruction of the interactions between them. During solution and simulation process using PD theory, no new bond is created between the material points of the body, and if the relative change in the length of the bond vector between the two material points x and x' in the body exceeds a specified limit, called the critical relative change in the length of the bond vector between the material points (s_0), the bond between them is broken, and hence, the interaction between the two points of material is eliminated and the damage in material occurs.

Regarding the concept of damage in PD theory and the above-mentioned issues, the pairwise force function in the bond vector between material points is defined as relation (16):

$$\boldsymbol{f(\eta,\xi) = \frac{\xi+\eta}{|\xi+\eta|} cs\mu(t,|\xi|)} \tag{16}$$

In relation (16), $\mu(t,|\xi|)$ is a time-dependent scalar function defined as follows:

$$\boldsymbol{\mu(t,\xi) = \begin{cases} 1, & s(t\ ,\xi) < s_0 \\ 0, & otherwise \end{cases}} \tag{17}$$

The relationship between the pairwise force in the bond vector between the material points and the change in the length of bond vector between them and also the relationship between the damage factor ($\mu(t,\xi)$) between the material points and the length of bond vector changes between them are shown in figure (3).Then, we write:

$$\boldsymbol{f(\eta,\xi) = \begin{cases} \frac{\xi+\eta}{|\xi+\eta|} cs, & s(t\ ,\xi) < s_0 \\ 0\ , & otherwise \end{cases}} \tag{18}$$

The concept of the local damage and failure for any material point x in PD theory is defined as follows:

$$\boldsymbol{\varphi(x,t) = 1 - \frac{\int_{\mathcal{H}_x} \mu\ (x,t,\xi) dv_\xi}{\int_{\mathcal{H}_x} dv_\xi}} \tag{19}$$

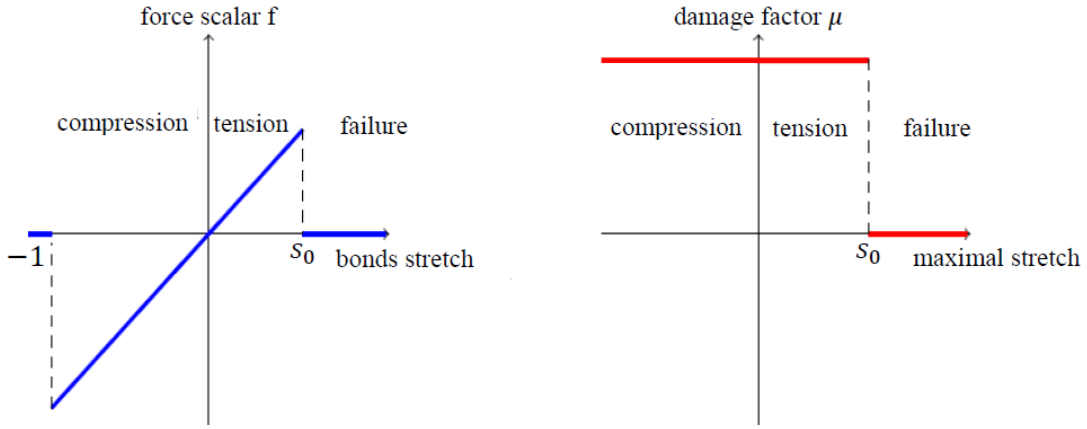

Fig. 3. Variation of interparticle force with bond stretching factor and damage factor changes with maximum bond stretching.

Since relation (17) changes the value of $\mu(t,|\xi|)$ between 0 and 1, the value of $\varphi(x,t)$ in relation (19) varies between 0 and 1. Indeed, the value of 0 for the function $\varphi(x,t)$ indicates that the all bonds connected to the material point x are intact and the value of 1 indicates that all the bonds

connected to the material point *x* are failed and disappeared. It should be noted that in this study, the value of the local damage index (φ) in PD theory was considered 0.38, that is, for crack growth, only 38% of the bonds between a material point and another point in its neighborhood must be eliminated, so that separation occurs in the material with the crack propagation and failure.

The concept of the local damage in PD theory is shown in **Fig 4.**

(a): $\boldsymbol{\varphi = 0}$ (b): $\boldsymbol{\varphi = 1}$

Fig. 4. Schematic of local damage for material point *x*.

3 Numerical scheme of PD theory

The numerical solution of equation (2) is performed in PD theory using mesh less method. In this method, the whole body is first divided into nodal points, each node having a specific volume in the reference configuration. The size of the nodes can be non-uniform, for simplicity, the nodes are considered to be a cube with the side length Δx. Indeed, Δx is the longitudinal or transverse distance of the material points in PD theory. The discrete form of equation (2) in PD theory using the midpoint integral rule is as follows [15]:

$$\boldsymbol{\rho \ddot{u}_i = \sum_j f\left(u_j{}^n - u_i{}^n, x_j - x_i\right) V_j + b_i{}^n} \tag{20}$$

As in relation (20), $u_i{}^n = u(x_i, t^{\,n})$ is the displacement of the i-th node at the time $t^{\,n}$, where *n* is the time step number. In addition, in the above relation, V_j is the volume of the node *j*. It is worth noting that the node size in the two-dimensional and one-dimensional states is surface and length of the node, respectively. The left side of equation (20) can be replaced by the explicit central difference relation:

$$\boldsymbol{\ddot{u}_i{}^n = \frac{u_i{}^{n+1} - 2u_i{}^n + u_i{}^{n-1}}{\Delta t^2}} \tag{21}$$

To solve the differential part of equation (21), the Verlet velocity algorithm is used. This algorithm is as follows:

$$\begin{aligned} \boldsymbol{\dot{u}_{(k)}^{n+\frac{1}{2}}} &= \boldsymbol{\dot{u}_{(k)}^{n} + \frac{\Delta t}{2}\ddot{u}_{(k)}^{n}} \\ \boldsymbol{u_{(k)}^{n+1}} &= \boldsymbol{u_{(k)}^{n} + \Delta t\ \dot{u}_{(k)}^{(n+1)/2}} \\ \boldsymbol{\dot{u}_{(k)}^{n+1}} &= \boldsymbol{\dot{u}_{(k)}^{(n+1)/2} + \frac{\Delta t}{2}\ddot{u}_{(k)}^{n+1}} \end{aligned} \tag{22}$$

In the above relations, u, $\dot{u}$, and $\ddot{u}$ are respectively the displacement, velocity, and acceleration vectors. In fact, using the above relations, the acceleration, velocity, and displacement can be calculated for the k-th material point of the object.

3. 1 Properties of material

The material studied in this research is Duran glass 50, the mechanical properties of which are described in **Table 1**

Table 1. Material properties of Duran glass 50

Density (ρ)	Young's modulus (E)	Poisson ratio (ν)	Fracture energy (G_0)
2235 kg/m^3	65GPa	0.2	204 J/m^2

3.2 Crack growth in a rectangular plate with a horizontal pre-crack

In this section, to validate the code written in LAMMPS software to model crack growth using bond-based PD theory, dynamic crack growth is modeled on a rectangular plate with a horizontal pre-crack. In **Fig 5**, the flowchart related to the PD algorithm is drawn. The length and width of the rectangular plate are 100 mm and 40 mm, respectively. The geometry of the rectangular plate is shown schematically in **Fig 6**. According to this figure, the length of the horizontal pre-crack of the rectangular plate is a = 50 mm and the upper and lower boundaries of the body are subjected to uniform tensile stress of 12 MPa.

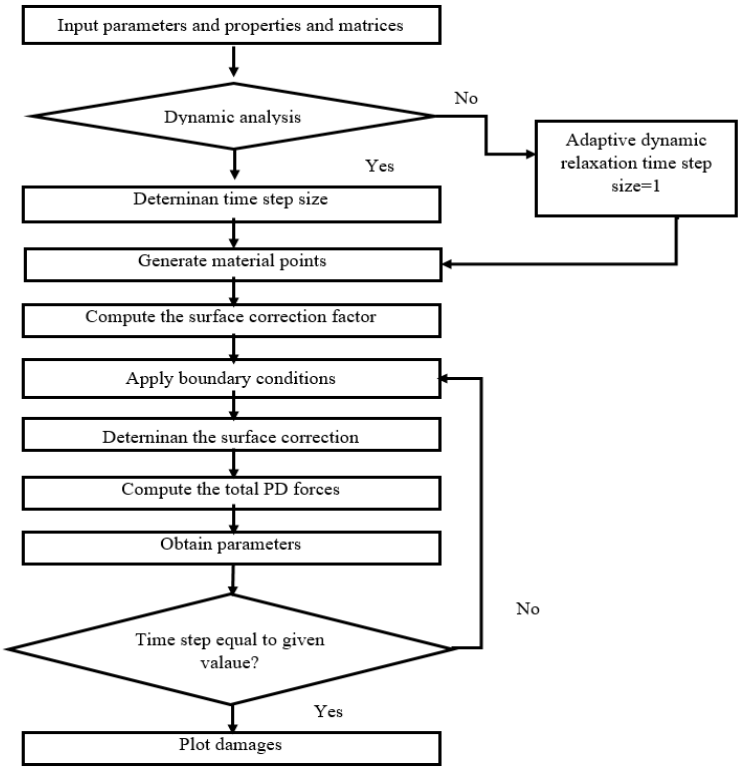

Fig. 5. Flowchart of PD theory.

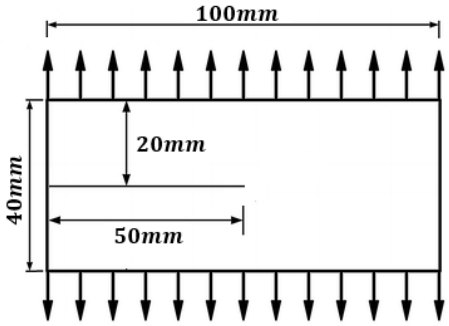

Fig. 6. Rectangular plate with a pre-crack.

In order to discretize the rectangular plate for crack growth analysis using PD theory, the plate is divided into square grids with side length Δx = 0.5 mm. In this study, the values of the horizon line and time step for modeling crack growth in the targeted rectangular plate using bond-based PD theory in LAMMPS software are considered δ = 4Δx and Δt = 50, respectively, according to the available references. The values of the micro module and critical tension parameters, according to the reference [10] for Duran glass50 material, are as follows: $c = 2.328\frac{10^{19}\mathrm{N}}{\mathrm{m}^5}$ and $s_0 = 0.001473$.

The results of crack growth modeling in the rectangular plate considered in this section are presented in **Fig 7**. The location and time of branching phenomenon in the crack path of the rectangular plate are mentioned in **Table 2** and in **Fig 8**, the result of crack growth modeling in this study is

compared with the results obtained in other references. According to **Table 2** and **Fig 8**, it is revealed that the code written in LAMMPS software to model crack growth using PD theory has high accuracy.

Table 2. Time and location of branching of the crack paths in the rectangular plate under the uniform stress of 12 MPa

	Branching position	Branching time
this research	19 mm	$25\mu s$
Ref [11]	19 mm	$25\mu s$
Ref [17]	25 mm	$28\mu s$

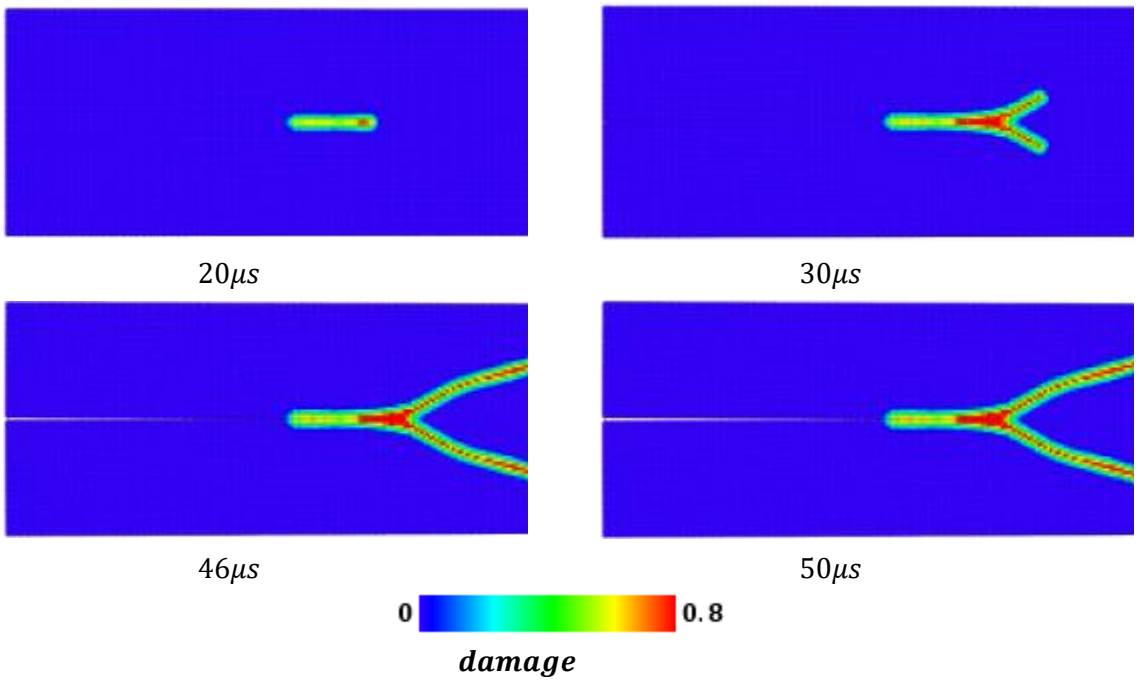

Fig. 7. Crack propagation path in the rectangular plate with a pre-crack under a uniform stress of 12 MPa

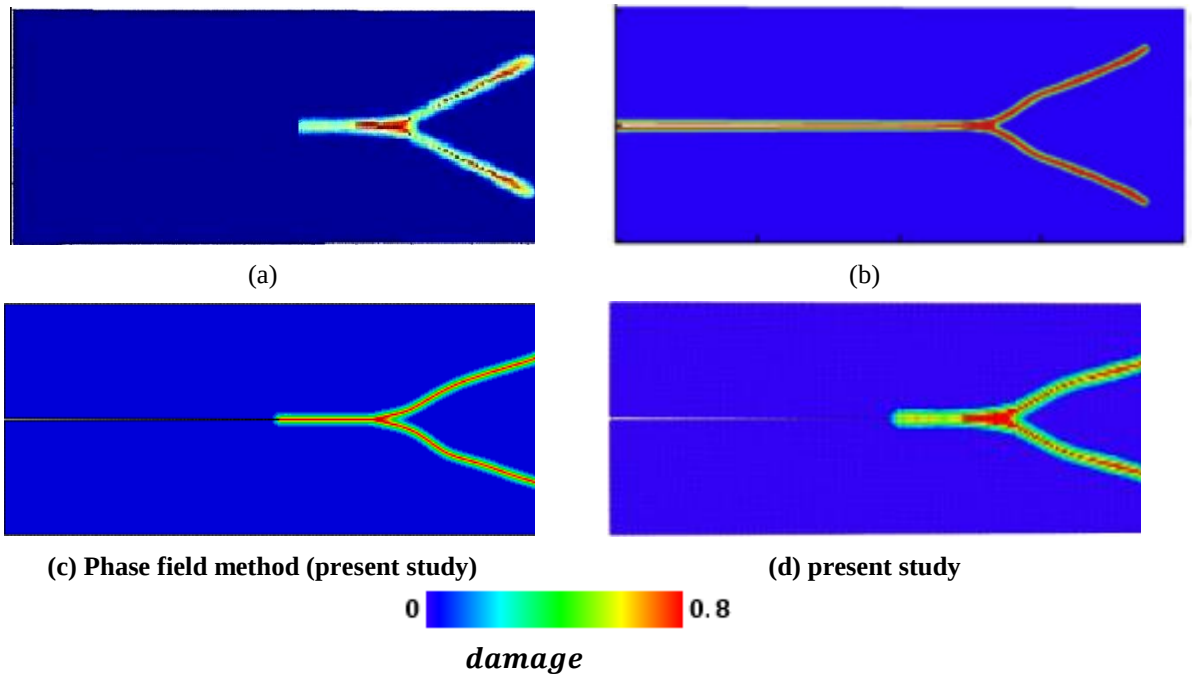

Fig. 8. Crack propagation path in the plate with a pre-crack subjected to a uniform stress of 12 MPa, a) Shafiei [17], b) Ha [11], c) Phase field method, d) present study**.**

3.3 Crack growth in unidirectional composite plate with a hole

Here, the crack growth is modeled in a single-layer unidirectional composite plate with a hole. Also, in order to investigate the effect of fiber angle on the propagation of crack in the composite plate, the crack growth is examined for fiber angles of 0 and 90 degrees. The geometry of the desired plate is shown in **Fig 9** and the results of this section are displayed in **Fig 10**. Also, in **Table 3**, the mechanical characteristics of reinforcing fibers are given in two directions of 0 and 90 degrees.

Table 3. Mechanical properties of unidirectional composite plate

ρ	G_0^{22}	G_0^{11}	v_{12}	E_{22}	E_{12}	E_{11}
1630 kg/m^3	0.168 kJ/m^2	15.49 kJ/m^2	0.346	6 GPa	4.4 GPa	329 GPa

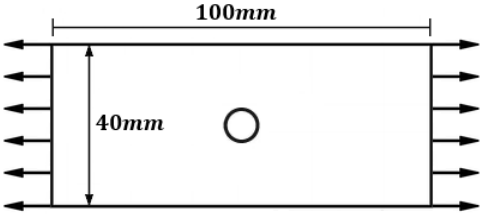

Fig. 9. Geometry of a single-layer unidirectional composite plate with a circular hole**.**

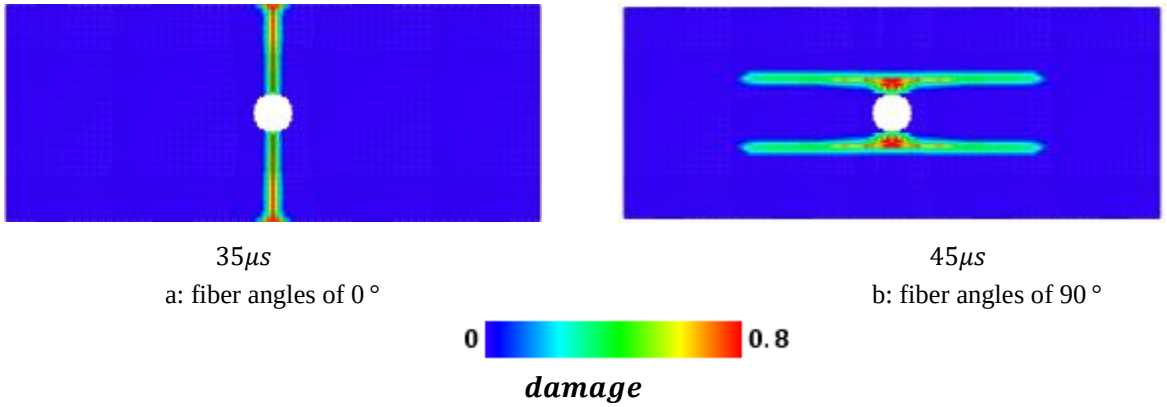

a: fiber angles of 0 °

b: fiber angles of 90 °

Fig. 10. Crack propagation path in the unidirectional composite plate: a: fiber angles of 0 °, b: fiber angles of 90 °.

According to the obtained results of this section, it is revealed that the fiber direction in the composite plate affects the manner of crack growth in it.

3.4 Crack growth in a rectangular bimaterial plate with a horizontal pre-crack

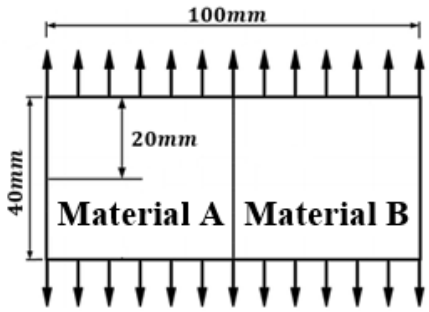

Fig. 11. Geometry of rectangular bi-material plate with a horizontal pre-crack under a uniform stress of 6 MPa.

Here, the crack growth is modeled in a rectangular bi-material plate with a horizontal pre-crack under uniform stress. The geometry of the desired plate is indicated in **Fig 11** and the results of this section are shown in **Fig 12**.

According to the results obtained in this section, it can be stated that the type of material of the body will affect the growth of cracks in it.

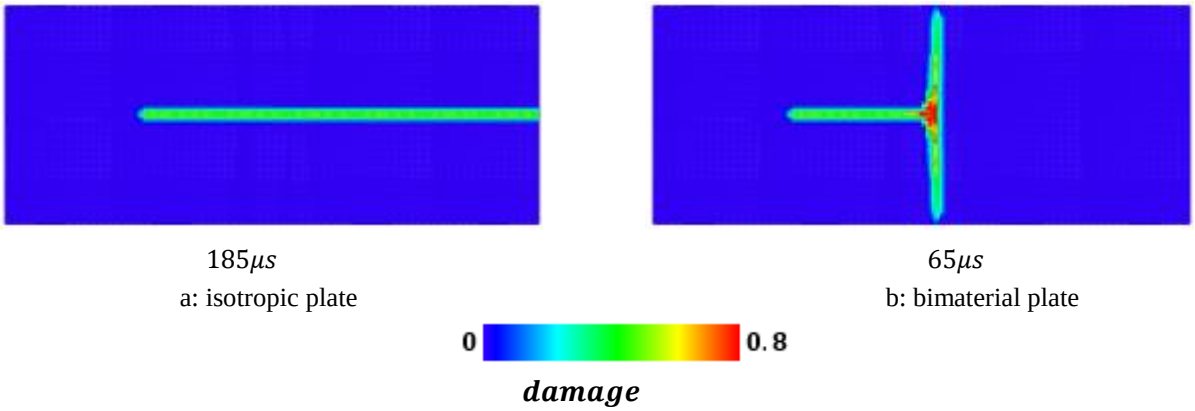

a: isotropic plate b: bimaterial plate

Fig. 12. Crack propagation path in: a: isotropic plate b: bi-material plate with a horizontal pre-crack**.**

3.5 Crack growth in a rectangular plate with hole and pre-crack

Here, the crack growth is modeled in a rectangular plate with a pre-crack and circular hole under uniform stress. The geometry of the desired plate is indicated in **Fig 13** and the results of this section are shown in **Fig 14**.

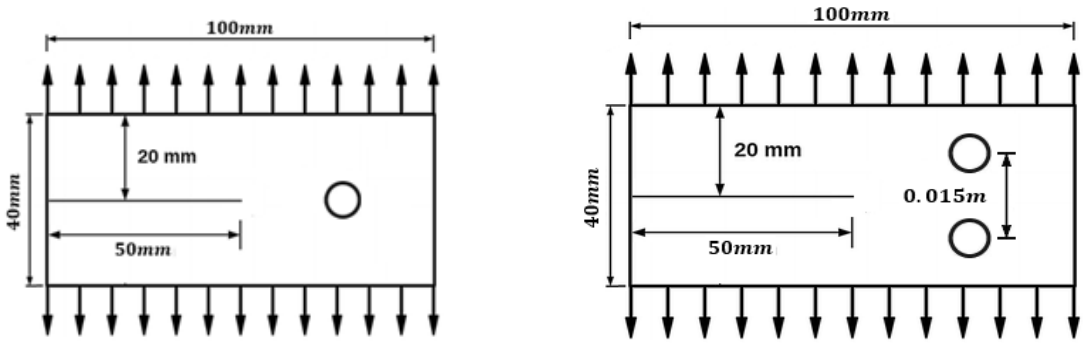

a:isotropic plate with a circular hole b:isotropic plate with two circular hole

Fig. 13. Geometry of isotropic plate with a horizontal pre-crack and circular hole under a uniform stress of 6 MPa.

According to the obtained results of this section, it is found that the number and location of holes in the body affect the crack growth in it.

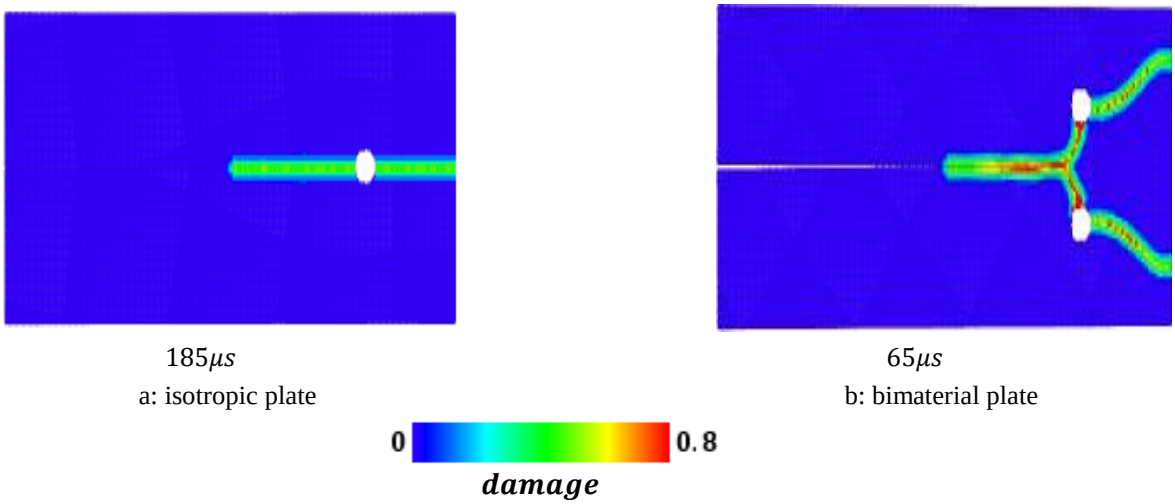

a: isotropic plate b: bimaterial plate

Fig. 14. Crack propagation path in: a: isotropic plate with a circular hole and pre-crack b: isotropic plate with two a circular hole and pre-crack.

3.6 Crack growth in a rectangular plate with pre-crack and inclusion

Here, the crack growth is modeled in a rectangular plate with a pre-crack and inclusion. The geometry of the desired plate and the inclusion in the body are shown in **Fig 15** and the results of this section are shown in **Fig 16**.

According to the obtained results of this section, it can be said that the presence of inclusion in the body has a significant effect on the manner of crack growth in it. In addition, the number and location of inclusions in the body affect the behavior of material and the growth of crack in it.

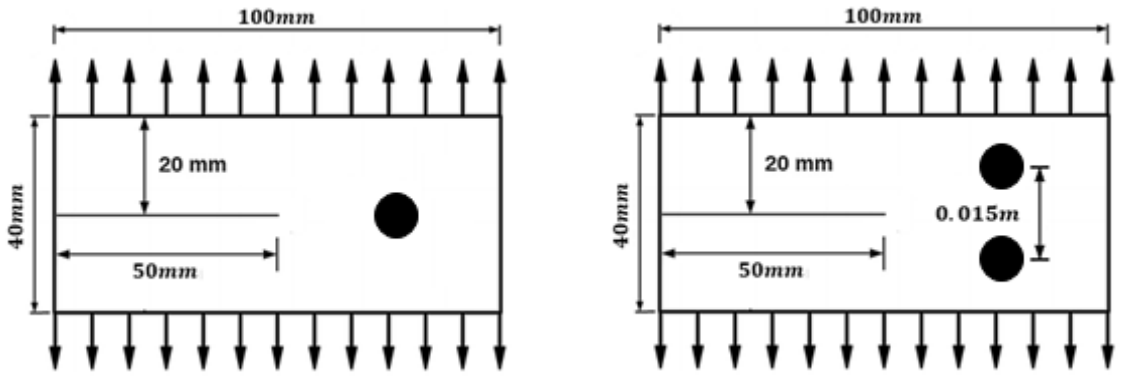

a:isotropic plate b: bimaterial plate

Fig. 15. Geometry of isotropic plate with a horizontal pre-crack and inclusion under a uniform stress of 6MPa**.**

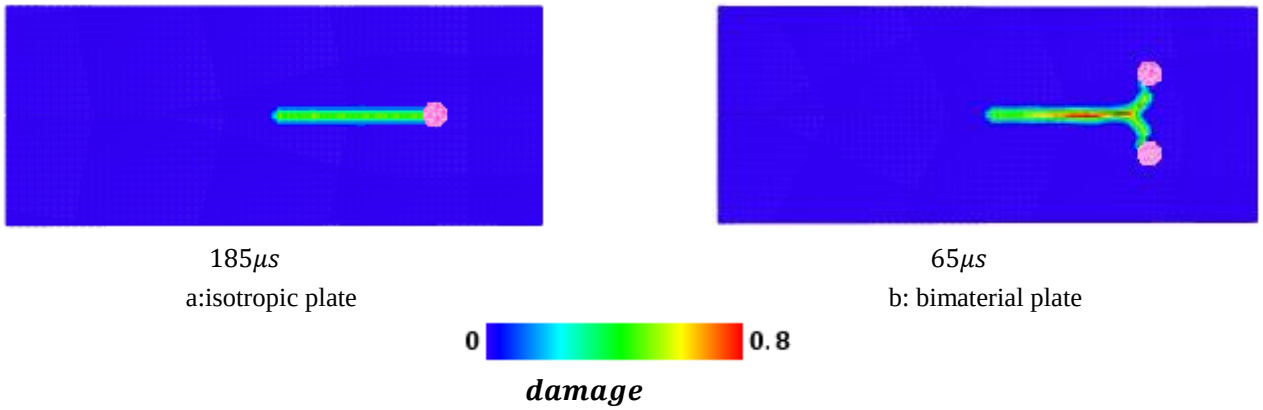

a:isotropic plate b: bimaterial plate

Fig. 16. Crack propagation path in: a: isotropic plate with a circular inclusion and pre-crack b: isotropic plate with two a circular inclusion and pre-crack.

4 Conclusions

In this study, dynamic crack growth was analyzed and modeled using the bond-based PD theory in LAMMPS software. The effect of some factors, including the applied stress value, type of material, fiber direction in composite plates, presence of inclusion, and number and location of holes in the body, on the crack initiation and propagation was also studied. In the first problem, the crack growth was modeled in a rectangular plate with a pre-crack of constant length under different stresses. According to the obtained results, the manner of crack growth in the body is highly dependent on the intensity of stress applied on it; as the stress value applied to the body increases, the material shows more brittle behavior and the crack grows more rapidly in several branches. In the second problem, the effect of fiber direction in composite plate on the crack propagation was investigated. According to the obtained results, it was found that the fiber direction has a great effect on the manner of crack growth in it. In the third problem, the crack growth was modeled in a bi-material rectangular plate with a horizontal pre-crack. According to the results of this part and the comparison of them with those of the first part, it was revealed that the type of material has a significant effect on the manner of crack growth in the body. In the fourth problem, the effects of the hole and inclusion in the body on the crack growth were

examined. The results displayed that the number and location of holes and the arrangement of inclusion in the body affect the crack growth in it. Also, according to the results of this section, under the same conditions, bodies with inclusion and bodies with hole differ greatly in the manner of crack growth and the behavior of material. Finally, according to the results of the present study, it is concluded that PD theory is able to analyze and predict the crack growth in different structural and loading conditions, using the same criteria, without the need for changing them. In addition, according to the obtained results, it is also revealed that how the crack propagates and branches in the body depends on the applied stress value, type of material, fiber direction in composite plates, and presence of inclusion in the body; so, as these factors change, the path, rate, and other parameters of the crack growth in bodies will change.

Acknowledgement

The authors would like to acknowledge and express their special gratitude to four anonymous reviewers for their constructive comments, which significantly improved the quality of the initial manuscript.

Funding Statement

The author(s) received no specific funding for this study.

CRediT authorship contribution statement

Mohammad Norouzi Shavir: Investigation, Formal analysis. **Pouria Biglari**: Conceptualization, Formal analysis, Writing–review & editing. **Navid Mirzaii**: Investigation, Writing–review & editing. **Reza Rashmehkarim**: Conceptualization, Investigation, Formal analysis, Writing–original draft. **Peyman Beiranvand**: Formal analysis, Writing–original draft, Writing editing, Investigation.

Conflicts of Interest

The authors declare no conflict of interest.

References

[1] Silling SA. Reformulation of elasticity theory for discontinuities and long-range forces. Journal of the Mechanics and Physics of Solids 2000; 48(1): 175–209. https://doi.org/10.1016/S0022-5096 (99)00029-0

[2] Diehl P, Prudhomme S, Lévesque M. A Review of Benchmark Experiments for the Validation of Peri-dynamics Models. Journal of Peridynamics and Nonlocal Modeling 2019; 1(1): 14–35. https://doi.org/10.1007/s42102-018-0004-x

[3] Javili A, Morasata R, Oterkus E, Oterkus S. Peri-dynamics review. Mathematics and Mechanics of Solids 2019; 24(11): 3714–3739. https://doi.org/10.1177/1081286518803411

[4] Madenci E, Oterkus E. Peridynamic Theory and Its Applications. Springer 2014; 19–43. https://doi.org/10.1007/978-1-4614-8465-3

[5] Silling SA, Askari E. A meshfree method based on the Peri-dynamic model of solid mechanics. Computers and Structures 2005; 83(17–18): 1526–1535. https://doi.org/10.1016/j.compstruc.2004.11.026

[6] Kilic B, Madenci E. Structural stability and failure analysis using Peri-dynamic theory. International Journal of Non-Linear Mechanics 2009; 44(8): 845–854. https://doi.org/10.1016/j.ijnonlinmec.2009.05.007

[7] Parks ML, Lehoucq RB, Plimpton SJ, Silling SA. Implementing Peri-dynamics within a molecular dynamics code. Computer Physics Communications 2008; 179(11): 777–783. https://doi.org/10.1016/j.c pc.2008.06.011

[8] Parks ML, Seleson P, Plimpton SJ, Silling SA, Lehoucq RB. Peridynamics with LAMMPS: A User Guide v0.3 Beta. Sandia National Laboratories 2011.

[9] Silling SA, Epton M, Weckner O, Xu J, Askari E. Peri-dynamic states and constitutive modeling. Journal of Elasticity 2007; 88(2): 151–184. https://doi.org/10.1007/s10659-007-9125-1

[10] Ren H, Zhuang X, Cai Y, Rabczuk T. Dual-horizon Peri-dynamics. International Journal for Numerical. Methods in Engineering 2016; 108(12): 1451–1476. https://doi.org/10.1002/nme.5257

[11] Ha YD, Bobaru F. Studies of dynamic crack propagation and crack branching with Peri-dynamics. International Journal of Fracture 2010; 162(1-2): 229–244. https://doi.org/10.1007/s10704-010-9442-4

[12] Bobaru F, Ha YD. Adaptive refinement and multiscale modeling in 2D Peri-dynamics. Journal for Multiscale Computational Engineering 2011; 9(6): 635–659. http://dx.doi.org/10.1615/IntJMultCompEng.2011002793

[13] Ha YD, Bobaru F. Characteristics of dynamic brittle fracture captured with Peri-dynamics. Engineering

Fracture Mechanics 2011; 78(6): 1156–1168. https://doi.org/10.1016/j.engfracmech.2010.11.020
[14] Agwai A, Guven I, Madenci E. Predicting crack propagation with Peri-dynamics: A comparative study. International Journal of Fracture 2011; 171(1): 65–78. https://doi.org/10.1007/s10704-011-9628-4
[15] Zhou XP, Wang YT. Numerical simulation of crack propagation and coalescence in pre-cracked rock-like Brazilian disks using the non-ordinary state-based Peri-dynamics. International Journal of Rock Mechanics and Mining Sciences 2016; 89: 235–249. https://doi.org/10.1016/j.ijrmms.2016.09.010
[16] Zhao J, Tang H, Xue S. Peri-dynamics versus XFEM: a comparative study for quasi-static crack problems. Frontiers of Structural and Civil Engineering 2018; 12(4): 548–557. https://doi.org/10.1007/s11709-017-0434-6
[17] Giannakeas IN, Papathanasiou TK, Fallah AS, Bahai H. Coupling XFEM and Peri-dynamics for brittle fracture simulation-part I: feasibility and effectiveness. Computational Mechanics 2020; 66(1): 103–122. https://doi.org/10.1007/s00466-020-01843-z
[18] Shafiei A. Dynamic crack propagation in plates weakened by inclined cracks: an investigation based on Peri-dynamics. Frontiers of Structural and Civil Engineering 2018; 12(4): 527–535. https://doi.org/10.1007/ s11709-018-0450-1
[19] Silling SA, Askari A. Peri-dynamic model for fatigue cracking. Sandia National Laboratories 2014.
[20] Basoglu MF, Zerin Z, Kefal A, Oterkus E. A computational model of Peri-dynamic theory for deflecting behavior of crack propagation with micro-cracks. Computational Materials Science 2019; 162: 33–46. https://doi.org/10.1016/j.commatsci.2019.02.032
[21] Karpenko O, Oterkus S, Oterkus E. Influence of Different Types of Small-Size Defects on Propagation of Macro-cracks in Brittle Materials. Journal of Peridynamics and Nonlocal Modeling 2020; 2(3): 289–316. https://doi.org/10.1007/s42102-020-00032-z
[22] Kulkarni SS, Tabarraei A. An ordinary state based Peri-dynamic correspondence model for metal creep. Engineering Fracture Mechanics 2020; 233. https://doi.org/10.1016/j.engfracmech.2020.107042
[23] Liu W, Yan K, Li JQ, Yang S. Peri-dynamics-based simulation of semi-circular bending (SCB) testing. Construction and Building Materials 2021; 268. https://doi.org/10.1016/j.conbuildmat.2020.121190
[24] Wang YT, Zhou XP. Peri-dynamic simulation of thermal failure behaviors in rocks subjected to heating from boreholes. International Journal of Rock Mechanics and Mining Sciences 2019; 117: 31–48. https://doi.org/10.1016/j.ijrmms.2019.03.007
[25] He D, Huang D, Jiang D. Modeling and studies of fracture in functionally graded materials under thermal shock loading using Peri-dynamics. Theoretical and Applied Fracture Mechanics 2021; 111. https://doi. org/10.1016/j.tafmec.2020.102852
[26] Yang Z, Yang SQ, Chen M. Peri-dynamic simulation on fracture mechanical behavior of granite containing a single fissure after thermal cycling treatment. Computers and Geotechnics 2020; 120. https://doi.org/10.1016/j.compgeo.2019.103414
[27] Hu YL, De Carvalho NV, Madenci E. Peri-dynamic modeling of delamination growth in composite laminates. Composite Structures 2015; 132: 610–620. https://doi.org/10.1016/j.compstruct.2015.05.079
[28] Hu YL, Yu Y, Wang H. Peri-dynamic analytical method for progressive damage in notched composite laminates. Composite Structures 2014; 108(1): 801–810. https://doi.org/10.1016/j.compstruct.2013.10.018
[29] Kilic B, Agwai A, Madenci E. Peri-dynamic theory for progressive damage prediction in center-cracked composite laminates. Composite Structures 2009; 90(2): 141–151.https://doi.org/10.1016/ j.com pstruct.2009.02.015
[30] Bang D. Peri-dynamic modeling of hyper elastic materials. The University of Arizona 2016.
[31] Weckner O, Nik Mohamed NA. Viscoelastic material models in Peri-dynamics. Applied Mathematics and Computation 2013; 219(11): 6039-6043. https://doi.org/10.1016/j.amc.2012.11.090
[32] Cheng Z, Liu Y, Zhao J, Feng H, Wu Y. Numerical simulation of crack propagation and branching in functionally graded materials using Peri-dynamic modeling. Engineering Fracture Mechanics 2018; 191: 13–32. https://doi.org/10.1016/j.engfracmech.2018.01.016
[33] Kilic B. Peri-dynamic theory for progressive failure prediction in homogeneous and heterogeneous materials. The University of Arizona 2008.
[34] Heo J, Yang Z, Xia W, Oterkus S, Oterkus E. Buckling analysis of cracked plates using Peri-dynamics. Ocean Engineering 2020; 214. https://doi.org/10.1016/j.oceaneng.2020.107817